Theor Appl Climatol (2013) 111:601–607
DOI 10.1007/s00704-012-0696-9

ORIGINAL PAPER

Quantifying the Multivariate ENSO Index (MEI) coupling to CO_2 concentration and to the length of day variations

A. Mazzarella · A. Giuliacci · N. Scafetta

Received: 9 April 2012 / Accepted: 7 June 2012 / Published online: 22 June 2012

Abstract The El Niño Southern Oscillation (ENSO) is the Earth's strongest climate fluctuation on inter-annual time scales and has global impacts although originating in the tropical Pacific. Many point indices have been developed to describe ENSO but the Multivariate ENSO Index (MEI) is considered as the most representative since it links six different meteorological parameters measured over the tropical Pacific. Extreme values of MEI are correlated to the extreme values of atmospheric CO_2 concentration rate variations and negatively correlated to equivalent scale extreme values of the length of day rate variation. We evaluate a first-order conversion function between MEI and the other two indexes using their annual rate of variation. The quantification of the strength of the coupling herein evaluated provides a quantitative measure to test the accuracy of theoretical model predictions. Our results further confirm the idea that the major local and global Earth–atmosphere system mechanisms are significantly coupled and synchronized to each other at multiple scales.

A. Mazzarella (✉) · A. Giuliacci
Meteorological Observatory, Department of Earth Science,
University of Naples Federico II,
Largo S. Marcellino 10,
80138 Naples, Italy
e-mail: adriano.mazzarella@unina.it

A. Giuliacci
Epson Meteo Center,
via de Vizzi 93/95,
20092 Cinisello Balsamo, Milan, Italy

N. Scafetta
Active Cavity Radiometer Irradiance Monitor (ACRIM) Lab,
Coronado, CA 92118, USA

N. Scafetta
Duke University,
Durham, NC 27708, USA

1 Introduction

El Niño–La Niña is the strongest quasi-oscillatory pattern observed in the climate system and it is coupled to numerous climatic systems. Numerous empirical and theoretical studies have attempted to discover its multivariate influences and to model it in general circulation models (see, for example, Graf and Zanchettin (2012) and the literature referred therein).

However, current general circulation models (GCMs) do not reproduce well the patterns observed in climatic data such as trends and cycles at multiple time scales (Douglass et al. 2007; Scafetta 2010, 2012b; Spencer and Braswell 2011). The models also fail to forecast the summer from the preceding winter and vice versa and are unable to accurately simulate and predict some important circulation phenomena such as the quasi biennial oscillations and the El Niño/La Niña–Southern Oscillation (ENSO). These major climate variations are supposed to be generated by a not-well-understood internal dynamics (Meehl et al. 2011), although a contribution from astronomical harmonic forcings cannot be excluded (Wang et al. 2012). In general, numerous uncertainties affect our understanding of climate dynamics (Curry and Webster 2011).

The climate system is made of a set of subsystems coupled to each other and behaves as a complex network of coupled nonlinear oscillators, which synchronize to each other (Tsonis et al. 2008; Wyatt et al. 2011). For example, Scafetta (2010, 2012a) has shown that all major global,

hemispheric, land, and ocean surface temperature records are characterized by no less than 11 common frequencies from a period of 5 to 100 years that match equivalent astronomical cycles of the heliosphere and terrestrial magnetosphere. Mazzarella and Scafetta (2012) have shown that the North Atlantic Oscillation Index, the global ocean temperature, length of day, and a record of historically observed mid-latitude auroras present common quasi 60-year oscillations since 1700, which also suggests an astronomical origin of major climatic oscillations. Many other examples stress the importance of studying and directly quantify the strength of coupling among alternative physical observables. Indeed empirical modeling of climate change might have higher predicting power than traditional analytical models. Once that the strength of the couplings among the climate subsystems is properly quatified, it may be possible to evaluate how well-proposed physical models can reproduce them. This testing process would eventually yield better and more accurate theoretical models.

Bacastow (1976) found that atmospheric carbon dioxide record is correlated to the Southern Oscillation Index (SOI), which indicates that a component of the change in the rate of CO_2 removal is regulated by the southern tropical wind and ocean oscillations. More recently, Zheng et al. (2003) concluded that ENSO events, the changes in the length of day (LOD), and the global atmospheric angular momentum are correlated. However, Bocastow and Zheng et al. simply evaluated the correlation coefficients between two records and their reciprocal time lag. However, a more quantitative relation would be more useful because it can be more directly used to test the accuracy of the models.

In the following, we study the relations among: the recent monthly data of Multivariate Enso Index (MEI) that measures the ENSO, which is the Earth's strongest natural climate fluctuation on inter-annual time scales; the atmospheric CO_2 concentration measured at Mauna Loa; and the LOD, which is a global astronomical observable phenomenon. We notice that MEI is a more comprehensive index than SOI and ENSO. We use a similar mathematical methodology to study the mutual correlation and to quantify it. Finally, we discuss possible underlying geophysical phenomena that could explain the findings.

2 Data collection

We have analyzed the monthly values of:

1. MEI (interval, 1950–2011) as computed by Wolter and Timlin (1993, 1998) (http://www.cdc.noaa.gov/people/klaus.wolter/MEI/table.html). The record is depicted in Fig. 1a. Each monthly value is based on bimonthly means; for example, the February 2000 value is calculated from January-February 2000 data (Wolter and Timlin 1993). MEI is a multivariate measure of the ENSO signal. It is the first principal component of six main observed variables over the tropical Pacific: sea level pressure, zonal and meridional components of the surface wind, sea surface temperature, surface air temperature, and cloudiness of the sky. The MEI monthly values are standardized with respect to a 1950–1993 reference period and are expressed as fractions of standard deviation for which it has a total mean equal to 0 and a standard deviation equal to 1.
2. CO_2 (ppm) monthly concentration data measured at Mauna Loa (lat. 19°32′10″ N; long. 155°34′34″ W; height, 3,397 m; interval, 1958–2011) (ftp://ftp.cmdl.noaa.gov/ccg/CO_2/trends/CO_2_mm_mlo.txt). The record is depicted in Fig. 1b.
3. LOD (ms), i.e., the difference between the astronomical length of day and the standard length (interval, 1962–2010) (Stephenson and Morrison 1995) (ftp://hpiers.obspm.fr/eop-pc/eop/eopc05/eopc05_daily). The record is depicted in Fig. 1c.

3 Methodology and results

3.1 Long-term analysis

The three curves depicted in Fig. 1 appear quite different from each other. The MEI index fluctuates in an irregular way around a zero average. The CO_2 concentration record presents a clear upward trend due to the addition of anthropogenic gases plus a smaller annual oscillation due to the physical asymmetry between the Northern and Southern hemispheres. The LOD decreases and presents a clear annual cycle plus an apparently cyclical modulation with period of about 18–20 years, which, perhaps, may be astronomically induced by the 18.6-year solar–lunar nodal cycle or other astronomical cycles (Douglass et al. 2007) (we do not discuss this issue further in this paper). The dynamical patterns observed in the original records depicted in the figure would suggest that the three records are strongly uncorrelated: the cross-correlation between MEI and CO_2 gives r=0.08; MEI–LOD gives r=0.01; CO_2–LOD gives r=−0.69, which is negative and large only because one record (CO_2) has an upward trend and the other (LOD) has a downward trend during the given period. The parameters of the mean square regression line for the three records on time are summarized in Table 1.

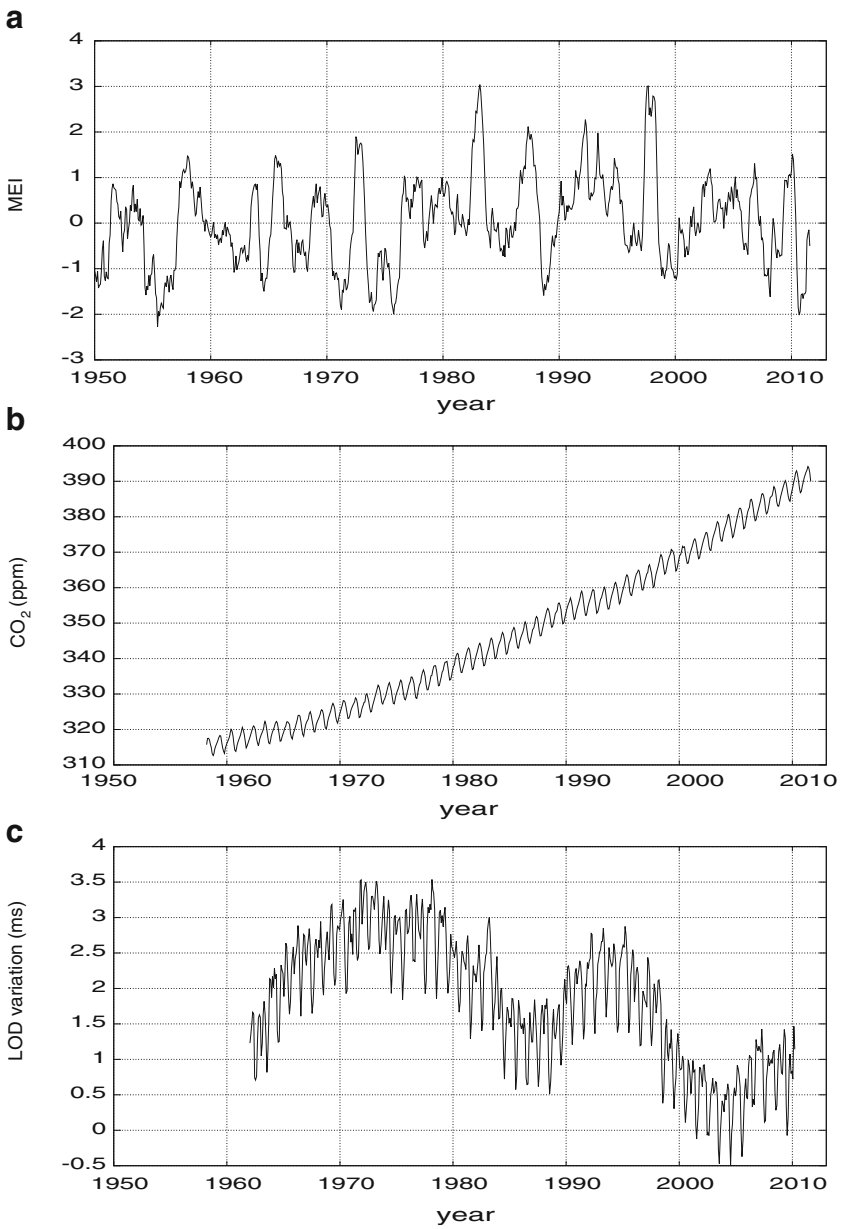

Fig. 1 **a** Time plot of monthly MEI values (interval, 1950–2011). **b** Time plot of monthly values of CO_2 measured at Mauna Loa (lat. 19°32′10″ N; long. 155°34′34″ W; height, 3,397 m; interval, 1958–2011). **c** Time plot of monthly LOD values (interval 1962–2010)

The above results would suggest that no simple relation exists among the three records.

3.2 Seasonal annual cycle analysis

MEI does not present any evident regular annual cyclical variability. Each of the six time series is "normalized by computing the bimonthly anomalies from the respective long term averages" (Wolter and Timlin 2011). On the contrary, both CO_2 and LOD present a clear annual cyclicity. LOD follows quite closely the annual cycle with maximum values during the winter and minimum values during the summer, while CO_2 annual cycle presents maximum values in the spring (April–June) and minimum values during September and October (see Fig. 2 where, for visual convenience, we compare the two records from 1978 to 1985).

Table 1 Parameters of mean square regression line of annual values of MEI, CO_2 and LOD on time, from 1962 to 2010, according to the function $Y(t)=m\ (t-1962)+n$

	m	n
MEI	0.012±0.003	−0.18±0.09
CO_2 (ppm)	1.48±0.01	309.7±0.3
LOD (ms)	−0.042±0.002	2.93±0.06

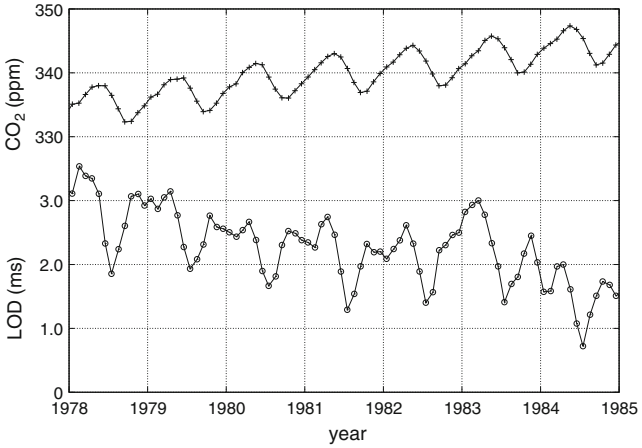

Fig. 2 Illustration of the annual cycle of LOD and CO_2 from 1978 to 1985; other time intervals are qualitatively equivalent. The CO_2 cycle lags the LOD annual cycle by about a season

The CO_2 annual cyclicity can be easily explained by the observation that from October to April the Northern Hemisphere (NH) cools while the Southern Hemisphere (SH) warms. Because most land is located in the NH while most ocean is located in the SH, the CO_2 atmospheric concentration is expected to increase from October to April because both the plants in the NH and the warmer ocean in the SH would uptake less CO_2 from the atmosphere. The opposite situation occurs from May to September.

The annual seasonal variation in LOD has been first extensively discussed by Lambeck (1980), who identified the variable zonal wind circulation as the cause of LOD seasonal cycle. The annual LOD cyclicity is related to the annual temperature cycle. In fact, during the Northern Hemisphere winter, the Earth is at its closest distance from the sun and the incoming total solar irradiance is on average about 40 W/m^2 larger than during the summer. So, perhaps, during winter the overall temperature of the entire planet (ocean plus atmosphere) increases, causing a change in wind velocities that may result in exchanges of angular momentum between the atmosphere and the Earth (Rosen and Salstein 1985). LOD also presents a clear 6-month cycle that is a sub-harmonic of the annual cycle that may be related to the solar semiannual tidal harmonics whose detailed analysis is left to another study.

3.3 Annual rate variation analysis

The lack of a linear correlation among the three variables should not be taken to mean that these variables are not coupled. Indeed a strong coupling may exist, but it is simply nonlinear. Herein, we investigate whether a better correlation exists among MEI, LOD, and CO_2 using their annual rate variation function.

We proceed in the following way: First, we process the signals by eliminating the large seasonal variations identified in CO_2 and in LOD by annually differentiating the signals. That is, we compute the difference between the value of January 1963 and that of January 1962, between the value of February 1963 and that of February 1962, and so on for each month and for each year. The value is centered in the average of the chosen interval: for example, the difference between Jan/1963 and Jan/1962 will be centered in 0.5*(1963.04+1962.04)=1962.54. At the end, we obtain a monthly series of CO_2 and LOD annual rate variation. Figure 3a depicts the time plot of MEI and CO_2 annual rate variation record. Figure 3b depicts the time plot of MEI and LOD annual rate variation record. The processed MEI index is rescaled by using the linear conversion relation depicted in Fig. 4.

We observe a very good correlation among the extreme values, such as during the strong El Niño event of 1998. Note the good synchrony occurring during the El Niño events such as in 1965, 1972, 1983, 1987, and 1998 and with corresponding La Niña events.

In the figure, CO_2 lags MEI by 3 months (best correlation coefficient, r=0.49), while LOD lags MEI by 4 months (best correlation coefficient, r=−0.34). Both correlation coefficients are highly significant ($P(|r|>|r_0|)<0.01$). This result would suggest that LOD and CO_2 rate changes are driven by MEI oscillations.

It appears that, 3 months after all El Niño events, the CO_2 rate reaches a peak with the exception of the interval around 1991, and all La Niña events are followed by lowest values of CO_2. A similar argument can be repeated for the LOD annual rate index.

To explain the absence of synchrony around 1991, it is worth noting that a violent eruption of Mount Pinatubo (15°08′30″ N; 120°21′00″ E; 1,745 m asl), located in the same tropical latitude and upwind of Mauna Loa, began in June 1991. It was the second largest eruption of the twentieth century and has been classified with a Volcanic Explosivity Index of 6. For a few years after a major volcanic eruption (i.e., when there is an abundance of sulphate aerosols in the atmosphere), heterotrophic respiration decreases due to a lowering of the Earth's surface temperature and the productivity of forest ecosystems increases under enhanced diffuse radiation. Both processes lead to a negative anomaly in CO_2 growth rate that may explain the absence of synchrony between MEI and CO_2 in the 1991–1993 interval (Patra et al. 2005).

Figure 4a, b shows scatter graphs of the MEI index against the CO_2 and LOD annual rate variations, respectively.

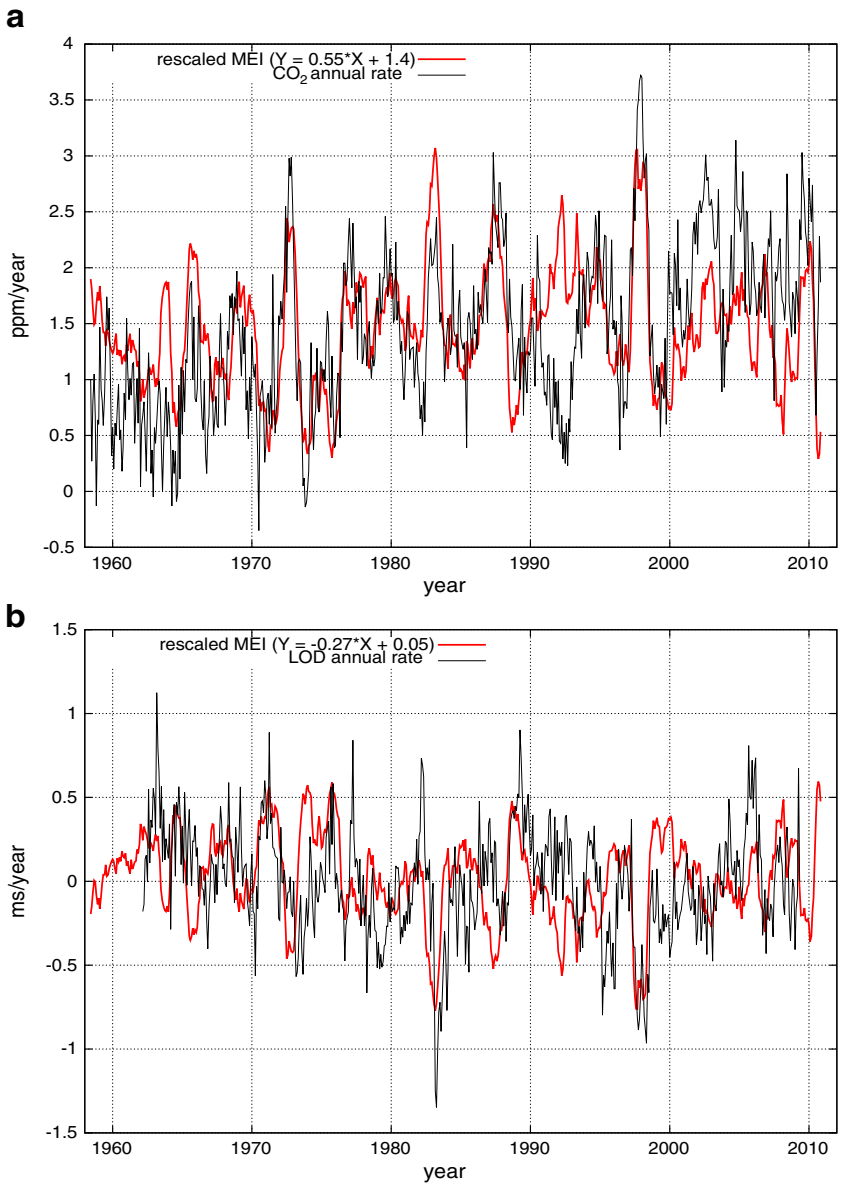

Fig. 3 **a** Time plot of rescaled MEI index (*red line*) and of CO_2 annual rate variation. The CO_2 curve is shifted 3 months back for best correlation. **b** Time plot of MEI (*red line*) and of LOD annual rate, which is shifted 3 months back for best correlation. Note that in b the MEI record is not only rescaled but also flipped upside-down to visually help a reader to notice its good correlation with LOD annual rate. The CO_2 and LOD curves are plotted against a rescaled MEI index according to the scatter graph results depicted in Fig. 4. Note the good correlation between the depicted curves where the larger minimum and maximum extremes usually correspond

Figure 4a suggests that, in first-order approximation, the CO_2 annual rate variation can be obtained from MEI by approximately multiplying the latter by K=0.55 ppm/year. Figure 4b suggests that, in first approximation, the LOD rate variation can be obtained from MEI by approximately multiplying the latter by K=−0.27 ms/year. The two first-order conversion functions are depicted in Fig. 4a, b and are used to prepare the graphical comparisons depicted in Fig. 3a, b.

4 Discussion and conclusions

ENSO is the Earth's strongest natural climate fluctuation on inter-annual time scales. It is a complex atmospheric and oceanographic phenomenon that has profound economic and social consequences (Wang and Fiedler 2006). However, ENSO is best described by MEI that combines six representative meteorological variables measured in the tropical Pacific.

Current GCMs are not able to reproduce or forecast ocean oscillations such as ENSO events. This failure may be due to a poor understanding of the ocean oscillations, their physical mechanisms, and true forcings (Scafetta 2010, 2012c; McLean 2009). It has been proposed that ENSO is, at least to some degree, a stable mode or oscillation triggered by random disturbances (Philander and Fedorov 2003). ENSO oscillations may also be interpreted in terms of a self-organized critical state (Mazzarella and Giuliacci 2009). However, complex astronomical and tidal cyclical

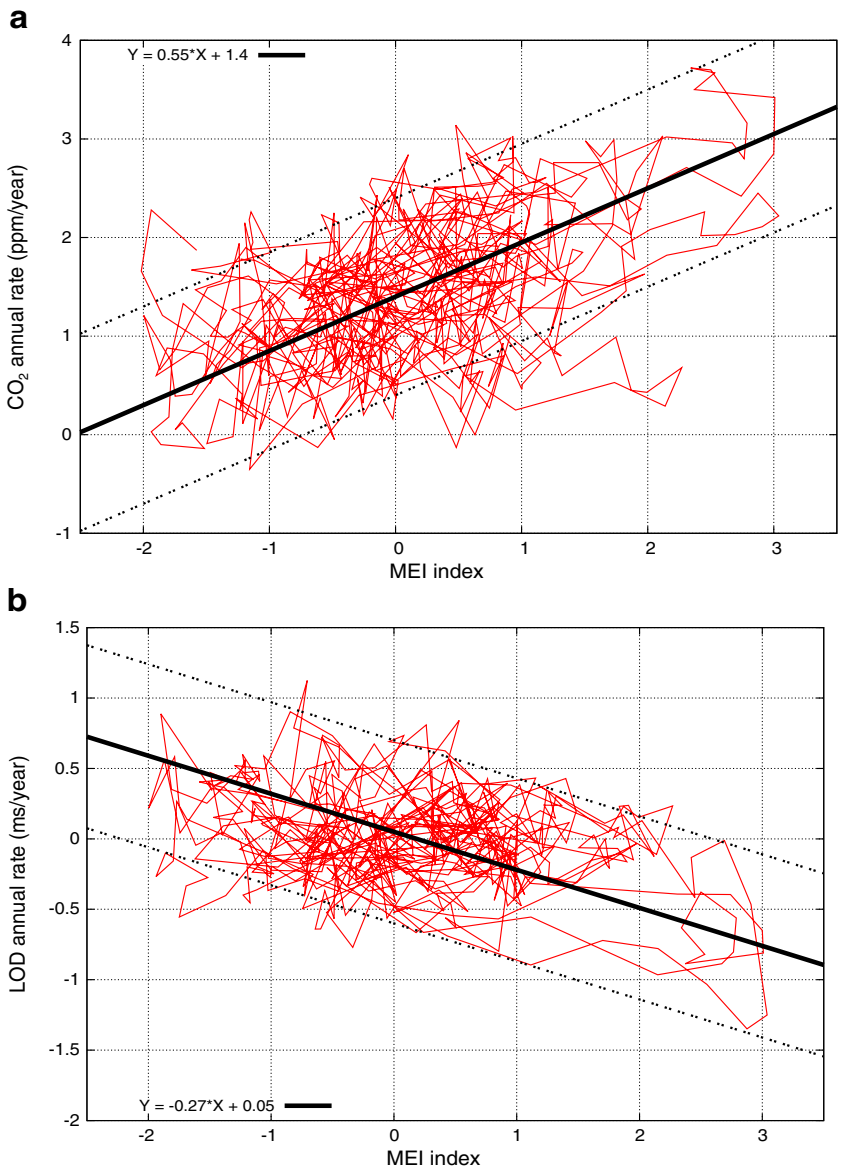

Fig. 4 **a** Scatter graphs of the MEI index against the annual rate of CO_2 (the CO_2 rate index is shifted back by 3 months). **b** Scatter graphs of the MEI index against the annual rate of LOD (the LOD rate index is shifted back by 4 months). The figures report also the proposed optimal first-order conversion functions that have been used in Fig. 3a, b, respectively

forcings, today ignored in the climate models, may be significantly involved in the process (Scafetta 2010, 2012a, 2012b; Wang et al. 2012). Thus, it is important to analyze the data in detail to identify all physical mechanisms that may be involved in the process.

Herein, we have studied three geophysical indexes: MEI, LOD, and CO_2 records. We have shown that the LOD and CO_2 annual rates are well correlated to MEI. In Fig. 4, we have quantified the conversion factors and showed the good agreement in Fig. 3.

The highest values of MEI show a direct and an inverse relationship with the highest values of CO_2 and LOD annual rate occurring after just a few months, respectively (Fig. 3). Since the highest values of MEI represent El Niño events, the results obtained here show the influence of El Niño on CO_2 and on LOD. It is worth noting that El Niño events occur in correspondence with an increase of sea surface temperature and a weakening of easterly trade winds (Wang and Fiedler 2006; Deser and Wallace 1990; Wallace 1998). But, a weakening of easterly winds causes an increase of zonal wind (Mazzarella 2008, 2009) that, like a torque, causes an acceleration of the Earth's rotation, i.e., a decrease of LOD. Equally, an increase of sea surface temperature causes a smaller solubility of CO_2 in the ocean and so a higher concentration in the atmosphere.

We propose that the nature and the magnitude of these correlations herein evaluated should be used to validate any analytical model attempting to reproduce the climate system in its effects and components.

References

Bacastow RB (1976) Modulation of atmospheric carbon dioxide by the Southern Oscillation. Nature 261:116–118

Curry JA, Webster PJ (2011) Climate science and the uncertainty monster. Bull Am Meteorol Soc. doi:10.1175/2011BAMS3139.1

Deser C, Wallace JM (1990) Large-scale atmospheric circulation features of warm and cold episodes in the tropical Pacific. J Climate 3:1254–1281

Douglass DH, Christy JR, Pearson BD, Singer SF (2007) A comparison of tropical temperature trends with model predictions. Int J Climatol. doi:10.1002/joc.1651

Graf H-F, Zanchettin D (2012) Central Pacific El Niño, the "subtropical bridge", and Eurasian climate. J Geophys Res 117:D01102

Lambeck K (1980) The Earth's variable rotation. Cambridge University Press, Cambridge, p 449

Mazzarella A (2008) Solar forcing of changes in atmospheric circulation, Earth's rotation and climate. Open Atmos Sci J 2:181–184

Mazzarella A (2009) Sun–climate linkage now confirmed. Energy Environ 20:123–130

Mazzarella A, Giuliacci A (2009) The El Niño events: their classification and scale-invariance laws. Ann Geophys 52:517–522

Mazzarella A, Scafetta N (2012) Evidences for a quasi 60-year North Atlantic Oscillation since 1700 and its meaning for global climate change. Theor Appl Climatol 107:599–609

McLean JD, de Freitas CR, Carter RM (2009) Influence of the Southern Oscillation on tropospheric temperature. J Geophys Res 114: D14104. doi:10.1029/2008JD011637

Meehl G, Arblaster J, Fasullo J, Hu A, Trenberth K (2011) Model-based evidence of deep-ocean heat uptake during surface-temperature hiatus periods. Nat Clim Chang. doi:10.1038/nclimate1229

Patra PK, Maksyutov S, Nacazawa T (2005) Analysis of atmospheric CO_2 growth rates at Mauna Loa using CO_2 fluxes derived from an inverse model. Tellus 57B:357–365

Philander SG, Fedorov A (2003) Is El Niño sporadic or cyclic? Annu Rev Earth Planet Sci 31:579–594

Rosen RD, Salstein DA (1985) Contribution of stratospheric winds to annual and semiannual fluctuations in atmospheric angular momentum and the length of day. J Geophys Res 90(D5):8033–8041

Scafetta N (2010) Empirical evidence for a celestial origin of the climate oscillations and its implications. J Atmos Solar-Terr Phys 72:951–970

Scafetta N (2012a) A shared frequency set between the historical mid-latitude aurora records and the global surface temperature. J Atmos Solar-Terr Phys 74:145–163

Scafetta N (2012b) Testing an astronomically based decadal-scale empirical harmonic climate model versus the IPCC (2007) general circulation climate models. J Atmos Solar-Terr Phys 80:124–137

Scafetta N (2012c) Multi-scale harmonic model for solar and climate cyclical variation throughout the Holocene based on Jupiter–Saturn tidal frequencies plus the 11-year solar dynamo cycle. J Atmos Solar-Terr Phys 80:296–311

Spencer RW, Braswell WD (2011) On the misdiagnosis of surface temperature feedbacks from variations in Earth's radiant energy balance. Remote Sens 3:1603–1613

Stephenson FR, Morrison LV (1995) Long-term fluctuations in Earth's rotation: 700 BC to AD 1990. Phil Trans R Soc A 35:165–202

Tsonis AA, Swanson KL, Wang G (2008) On the role of atmospheric teleconnections in climate. J Climate 21:2990–3001

Wallace JM (1998) On the structure and evolution of ENSO-related climate variability in the tropical Pacific: lessons from TOGA. J Geoph Res 103:14,241–14,259

Wang C, Fiedler PC (2006) ENSO variability and the eastern tropical Pacific: a review. Prog Oceanogr 69:239–266

Wang Z, Wu D, Song X, Chen X, Nicholls S (2012) Sun–moon gravitation-induced wave characteristics and climate variation. J Geophys Res 117:D07102

Wolter K, Timlin MS (1993) Monitoring ENSO in COADS with a seasonally adjusted principal component index. Proceedings of the 17th Climate Diagnostics Workshop, Norman, OK, NOAA/N MC/CAC, NSSL, Oklahoma Climate Survey, CIMMS and the School of Meteorology, University of Oklahoma, pp 52-57

Wolter K, Timlin MS (1998) Measuring the strength of ENSO events —how does 1997/98 rank? Weather 53:315–324

Wolter K, Timlin MS (2011) El Niño/Southern Oscillation behaviour since 1871 as diagnosed in an extended multivariate ENSO index (MEI.ext). Intl J Climatol 31:1074–1087

Wyatt MG, Kravtsov S, Tsonis AA (2011) Atlantic Multidecadal Oscillation and Northern Hemisphere's climate variability. Clim Dyn. doi:10.1007/s00382-011-1071-8

Zheng DW, Ding X, Zhou Y, Chen Y (2003) Earth rotation and ENSO events: combined excitation of interannual LOD variations by multiscale atmospheric oscillations. Glob Planet Chang 36:89–97